Journal of Applied Electrochemistry **32**: 725–733, 2002.

Recycling kraft pulping chemicals: cyclic voltammetry of molten salt mixtures containing Na_2CO_3, Na_2SO_4, Na_2S/Na_2S_x and Na_2O/Na_2O_2

R. WARTENA[1], J. WINNICK[1,*] and P.H. PFROMM[2,*]
[1]*School of Chemical Engineering, Georgia Institute of Technology, Atlanta, GA, USA 30332*
[2]*Institute of Paper Science and Technology, Atlanta, GA, USA, 30318; Currently: Department of Chemical Engineering, Kansas State University, Manhattan, KS, USA, 66506*
*(*authors for correspondence)*

Received 31 July 2001; accepted in revised form 16 April 2002

Key words: carbonate, electrolysis, kraft process, pulping

Abstract

Cyclic voltammetry (CV) has been used to investigate molten salt mixtures in the temperature range of 820–840 °C between the initial and anticipated final compositions for the proposed electrolytic recausticizing process of inorganic pulping chemicals. A mixture simulating the initial conditions for the proposed process (sodium carbonate, sodium sulfide/polysulfide and sodium sulfate) exhibited carbonate oxidation and sulfate reduction at the limits of the potential window. Additional oxidation of sulfide to sulfur occurs at potentials inside the positive limit of the potential window with subsequent chemical reaction to form polysulfide. To simulate the final composition sodium oxide and peroxide were added to the mixtures; the resulting CVs had an additional oxidation peak attributed to oxide and peroxide oxidation. We conclude the electrolytic recycle process is feasible, producing sulfide and oxide from carbonate and sulfate of sodium in the molten state, yet separation is necessary between the anolyte and catholyte so the reduction products are not consumed by oxidation.

1. Introduction

More than fifty million tons of kraft pulp are produced every year in the United States alone [1]. This process requires approximately twenty-eight million tons of inorganic pulping chemicals that need to be recycled. The overall process is termed 'kraft chemical recovery cycle' (Figure 1, A) [2]. We have developed a concept for an alternative to the conventional recausticizing operation by applying electrolysis to the inorganic molten salt mixture present at the bottom of the kraft recovery boiler (Figure 1, B). This could simplify the recausticizing process, remove the problems created by impurities in replacement lime, supply an avenue to incremental recausticizing capacity, and would conserve energy. The model starting reactants for our work are molten sodium carbonate, sodium sulfide and sodium sulfate. A successfully converted molten salt mixture would contain mainly sodium oxide (converted to sodium hydroxide when dissolved in water) and sodium sulfide/polysulfide.

Our prior investigation into the carbonate–sulfate system [3] demonstrated the decreased potential window with respect to a pure molten sodium carbonate system (1.7 V vs 2.6 V). The oxidation remained the same as in the pure carbonate system, carbonate oxidation to carbon dioxide and oxygen (Equation 1):

$$CO_3^{2-} \rightarrow CO_2 + \tfrac{1}{2}O_2 + 2\,e^- \qquad E^\circ_{900\,^\circ C} = 0\,V \qquad (1)$$

yet the cathodic reaction was determined to be a multistep sulfate reduction occurring at potentials less negative than sodium or carbonate reduction.

Here, we have performed cyclic voltammetry on synthetic mixtures resembling initial, intermediate, and near-final melts in our process concept. The present investigation focuses on the following systems:

(i) sodium carbonate and sulfide where sulfate results from contamination of the initial chemicals and *in situ* oxidation (this will be referred to as an initial melt)
(ii) initial melt with oxide additions
(iii) melts near the final target conversion which have been synthetically composed to be high in oxide and sulfide and low in carbonate and sulfate.

The purpose of this paper is to describe the electrochemical reductions and oxidations occurring at the limits of the potential window of the systems described above as well as the reactions at intermediate potentials and the associated chemical reactions. The voltammograms also provide identifying fingerprints for the reactions occurring in the melts as well as its composition and hence the conversion.

1.1. *Electrochemical reactions*

To interpret the cyclic voltammograms we have applied free energy calculations to determine standard potentials

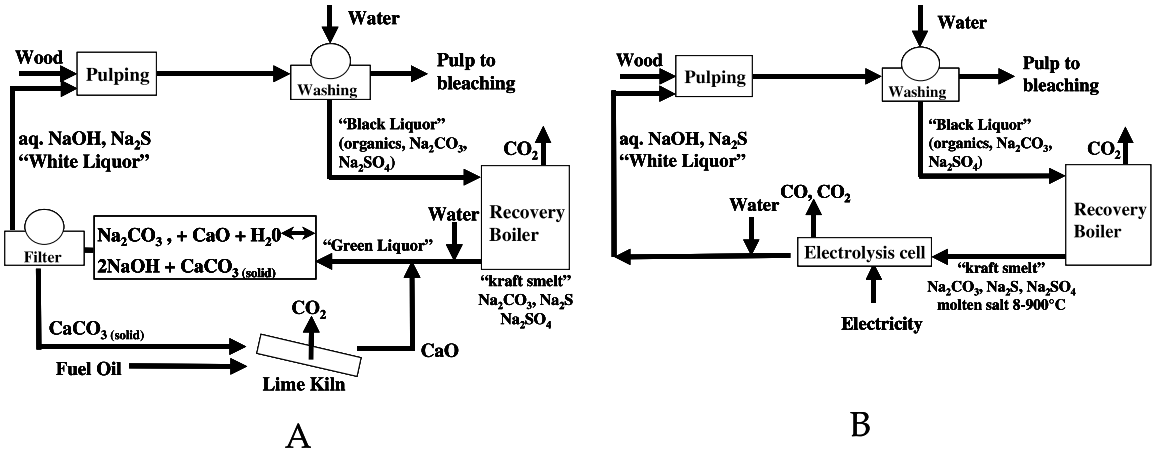

Fig. 1. A: Conventional kraft chemical recovery cycle B: Kraft chemical recovery via molten salt electrolysis (only main chemicals and reactions shown).

(assuming unit activity/ideal solution) of electrochemical reactions in conjunction with the literature for the electrochemistry of single and binary component systems.

1.1.1. *Thermodynamics*

All standard potentials ($E°$) presented are in reference to the carbonate–carbon dioxide–oxygen system (Equation 1). The standard potential is related to the free energy of reaction by,

$$\Delta g^{\circ}_{rxn} = -nFE^{\circ}_{rxn} \tag{2}$$

The standard potentials are evaluated with unit activity of all species (ideal solution) at 900 °C in the theoretical analysis and are based on the JANAF tables [4], Bureau of Mines Bulletin [5] and values provided elsewhere in the literature. The operating temperatures in the experiments were ~60 °C lower than the temperature at which the standard potential was evaluated corresponding to an increase in the standard potential of approximately 0.03 V.

1.1.2. *Electrochemistry of the individual compounds: sodium carbonate*

The relevant electrochemical characteristics of sodium carbonate were explored previously [3]. In the kraft smelt to be recycled, sodium carbonate has the largest concentration; its oxidation (Equation 1) occurs at the limit of the positive potential window in all systems investigated.

1.1.3. *Sodium sulfide*

Sodium sulfide is the second most abundant component of the kraft smelt to be recycled. The sulfide of sodium will not undergo any further reductions; however, it is possible for sulfide to oxidize to elemental sulfur:

$$S^{2-} \rightarrow \tfrac{1}{2}S_2 + 2\,e^- \qquad E^{\circ}_{900\,^{\circ}C} = -0.701\,V \tag{3}$$

Anodic sulfur production from sulfide is not detrimental because reaction with sodium sulfide leads to the immediate formation of sodium polysulfides, a desirable component in kraft pulping.

$$xS^{\circ} + S^{2-} \leftrightarrow S^{2-}_{x+1} \tag{4a}$$

$$\tfrac{1}{2}S_2 + Na_2S \leftrightarrow Na_2S_2 \qquad K_{900\,^{\circ}C} = 1.27 \times 10^2 \tag{4b}$$

The distribution of polysulfides has been well classified in the literature pertaining to the sodium-sulfur battery at much lower temperatures (~300 °C) [6]. Sulfide oxidation is anticipated at less positive potentials than carbonate oxidation (Equation 1) with currents proportional to reactant activity.

1.1.4. *Sodium oxide and sodium peroxide*

The sodium oxide reagent utilized in these investigations had a composition of 85 wt % Na_2O and 15 wt % Na_2O_2. We did not determine the compositional split between the different oxide species in our melts, although Andersen [7] reports a $51(O^{2-})$–$39(O_2^{2-})$–$10(\tfrac{1}{2}O_2^{-})$ mol % split between the oxides at about 927 °C under 1 atm oxygen in sodium carbonate. Sodium oxide will not undergo further reductions, but it is readily oxidized to either oxygen or peroxide, the reactions occurring at similar potentials:

$$O^{2-} \rightarrow \tfrac{1}{2}O_2 + 2\,e^- \qquad E^{\circ}_{900\,^{\circ}C} = -0.888\,V \tag{5}$$

$$2\,O^{2-} \rightarrow O_2^{2-} + 2\,e^- \qquad E^{\circ}_{900\,^{\circ}C} = -0.878\,V \tag{6}$$

When peroxide is present in the melt, it too may undergo oxidation to oxygen,

$$O_2^{2-} \rightarrow O_2 + 2\,e^- \qquad E^{\circ}_{900\,^{\circ}C} = -0.791\,V \tag{7}$$

1.1.5. *Sodium sulfate*

Sodium sulfate is present in kraft smelt due to incomplete reduction in the recovery boiler. In our experiments sodium sulfate is introduced into the system

through impurities in the carbonate and sulfide as well as developing from oxidation of sulfide by oxygen generated from the anodic reaction of carbonate (Equation 1):

$$Na_2S + 2\,O_2 \leftrightarrow Na_2SO_4 \qquad K_{900\,^\circ C} = 1.29 \times 10^{28} \tag{8}$$

The electrolytic reduction of sodium sulfate has been reported [8] at 927 °C through a sequence of two-electron transfers resulting in the formation of sodium sulfide and sodium oxide:

$$SO_4^{2-} + 2\,e^- \rightarrow SO_3^{2-} + O^{2-} \qquad E^\circ_{900\,^\circ C} = -1.822\,V \tag{9}$$

$$SO_3^{2-} + 2\,e^- \rightarrow SO_2^{2-} + O^{2-} \tag{10}$$

$$SO_2^{2-} + 2\,e^- \rightarrow \tfrac{1}{2}S_2^0 + 2O^{2-} \tag{11}$$

$$\tfrac{1}{2}S_2^0 + 2\,e^- \rightarrow S^{2-} \qquad E^\circ_{900^\circ C} = -0.701\,V \tag{12}$$

The sequence with steps of two electrons (Equation 9–12) will occur at potentials considerably less negative than the sodium and carbonate reductions:

$$Na^+ + 1\,e^- \rightarrow Na^0 \qquad E^\circ_{900\,^\circ C} = -2.19\,V \tag{13}$$

$$CO_3^{2-} + 2\,e^- \rightarrow 2\,O^{2-} + CO \qquad E^\circ_{900\,^\circ C} = -2.625\,V \tag{14}$$

The typical electrochemical oxidation at the edge of the potential window in pure sodium sulfate melts at 900 °C is the production of sulfur trioxide and oxygen [9],

$$SO_4^{2-} \rightarrow SO_3 + \tfrac{1}{2}O_2 + 2\,e^- \qquad E^\circ_{900\,^\circ C} = +1.203\,V \tag{15}$$

This will not occur in our systems of interest because oxidation of carbonate (Equation 1) will occur at potentials more than 1 V negative of sulfate oxidation. In conclusion, it is *not expected* for sulfate to participate in the electrochemical *oxidation*, yet it *is expected* to be electrochemically *reduced* to sulfide and oxide, while carbonate is chemically reduced by the intermediate sulfoxylate [3].

1.1.6. *Sodium carbonate and sodium sulfide*

In a melt containing sodium carbonate and sodium sulfide, the reactions occurring at the limits of the potential window are expected to be the same as those occurring in pure sodium carbonate, having a span of −2.6 V (Equations 1, 13 and 14), as long as carbonate has the dominant activity. Sulfide will not undergo further reduction; therefore sodium and carbonate ions will be the expected reduction reactants, as in a pure carbonate melt [3]. Carbonate will oxidize to carbon dioxide and oxygen (Equation 1) while sulfide will participate in the oxidation route to form polysulfides at less positive potentials (Equation 3). When the activity of sulfide is high with respect to carbonate, polysulfide formation is expected to consume a majority of the current at the limiting potentials.

1.1.7. *Sodium carbonate, sulfide, polysulfide and sulfate*

A mixture combining carbonate, sulfide (polysulfide) and sulfate is expected to exhibit electrochemical reactions at the limits of the potential window similar to a sodium carbonate and sodium sulfate mixture [3]. The anticipated span of such a voltammogram is about 1.7 V referring to the reduction of sulfate (Equations 9–12) and the oxidation of carbonate (Equation 1) with sulfide oxidizing to polysulfide (Equation 3) at less positive potentials.

1.1.8. *Sodium carbonate, sulfide, polysulfide, sulfate and oxide/peroxide*

With the addition of oxide and peroxide, the reactions occurring at the limits of the potential window are expected to be the same (span of ~1.7 V) as for the melt described in Section 1.1.7. but with the added oxidation reactions ascribed to the oxides (Equations 5–7). The purpose of this paper is not to identify the individual oxide oxidations but rather to determine if they occur. If oxide oxidation does occur it will be necessary to introduce a separator between the anode and cathode of the electrochemical cell to avoid consumption of the desired product.

2. Experimental details

2.1. *Apparatus*

2.1.1. *Electrochemical cell*

The cell was operated in a three-electrode configuration similar to that previously described [3]. A different electrode configuration was also used, when indicated, where the working (A, Figure 2) and the reference (B, Figure 2) were housed in a 61 cm long, 2.54 cm outer diameter 99.8% alumina closed end tube (C, Figure 2) (Vesuvius McDanel, Beaver Falls, PA); communication with the counter (D, Figure 2) in the bulk was maintained through a 0.051 cm diameter hole in the bottom of the tube (E, Figure 2). The hole was made through the 0.3 cm wall of the tube bottom by shaving 0.2 cm from the end with a diamond saw blade then drilling the hole with a tapered 0.0508 cm diamond-impregnated bit (Lunzer, Saddlebrook NJ). The density of the molten salt mixture was assumed to be 2.0 g cm^{-3} based upon the known densities of the individual components in the range of our operating temperature [10, 11]. Approximately 100 g of chemicals (Figure 2, F) were loaded into the crucible (Figure 2, G), and ~15 g (Figure 2, H) in the tube (Figure 2, C). The electrodes were all made from platinum wires (Alfa Aesar, Ward Hill MA). For

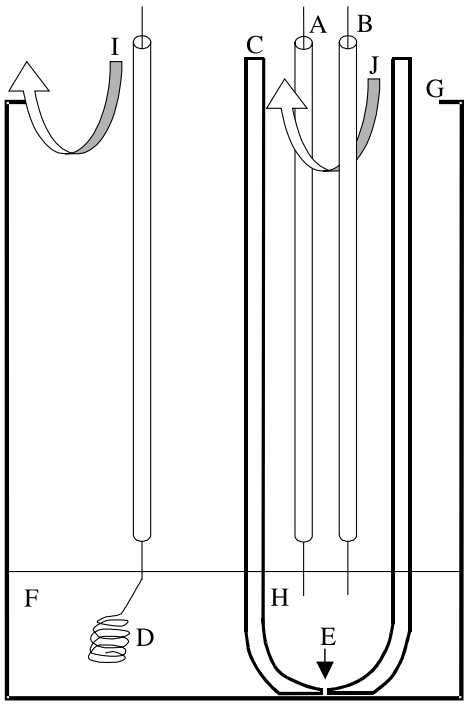

Fig. 2. Electrochemical cell. A: platinum working electrode; B: platinum reference electrode; C: alumina tube; D: platinum counter electrode; E: hole for communication between the working and the counter electrode; F: bulk molten salt of the counter electrode; G: alumina crucible; H: bulk molten salt of the working and reference electrode; I: purge of the counter electrode's chamber; J: purge of the working and reference electrode's chamber.

the initial melts and the initial melts with oxide additions, the working and counter electrodes were hammered flat. This was done to increase their surface area since the electrodes were also used for electrolysis experiments.

2.1.2. *Reference electrode*

The reference electrode was either a platinum wire behaving as a platinum sulfide electrode (Pt/PtS) (Equation 16) whose equilibrium depended upon the composition of the melt; or a mixed carbonate reference electrode (MCRE) (Equaiton 17):

$$\mathrm{Pt}\,|\,\mathrm{Na_2CO_3}, \mathrm{Na_2S_{(1,x)}}, (\mathrm{Na_2O/Na_2O_2}), \mathrm{Na_2SO_4}\,|\,\mathrm{Pt} \tag{16}$$

$$\mathrm{Pt}\,|\,\mathrm{Na_2CO_3}, \mathrm{Na_2S_{(1-x)}}, \mathrm{Na_2O/Na_2O_2}, \mathrm{Na_2SO_4}\,\Big|\,\begin{matrix}\text{Communication}\\ \text{hole}\end{matrix}\,\Big|\,(\mathrm{Li/Na})_2\mathrm{CO_3}\,|\,\mathrm{Pt} \tag{17}$$

For the melts with a composition similar to the initial kraft melt where oxide was added during the experiment, a three-electrode configuration was used: a platinum wire reference electrode was submerged in the molten salt mixture near the working electrode (Pt/PtS). Since the working and the reference were exposed to the same melt in the tube, separated from the counter electrode, the potential between the two was about 0 V. The reference reaction is either polysulfide or sulfide interacting with the platinum electrode:

$$2\,\mathrm{PtS} + 2\,\mathrm{e^-} \leftarrow 2\,\mathrm{Pt} + \mathrm{S_2^{2-}} \qquad E^\circ_{900\,^\circ\mathrm{C}} = -1.11\ \mathrm{V} \tag{18}$$

$$\mathrm{PtS} + 2\,\mathrm{e^-} \leftarrow \mathrm{Pt} + \mathrm{S^{2-}} \qquad E^\circ_{900\,^\circ\mathrm{C}} = -1.10\ \mathrm{V} \tag{19}$$

The reference cell for the MCRE contained a mixture of lithium and sodium carbonate such that the melting point of the reference would always be lower than that of the mixture under investigation. The reference gas above the melt was 0.05 to 0.1 L_{STP} min^{-1} of 14.7 vol % CO_2 and 2.94 vol % O_2 (balanced with nitrogen). The reference would exhibit a mixed behaviour between a carbonate reference electrode and a Pt/PtS when sulfide would diffuse into the reference chamber.

2.2. *Materials*

Sodium carbonate (anhydrous, granular, 99.5% assay, major impurity is sodium sulfate, VWR) and sodium sulfate (anhydrous, granular, 99.5% assay, VWR) were dried for 24 h in an oven at 115 °C. Sodium sulfide (89.8% purity determined by titration) was obtained from Alfa Aesar where the impurities included sodium sulfate, sulfur and sodium polysulfides as indicated by the slight yellow colour of the reactants received. Sodium oxide was also obtained from Alfa Aesar (manufacturer's assay 85 wt % Na_2O, 15 wt % Na_2O_2). Industrial grade argon (Air Products) served as the purge gas.

2.3. *Procedure*

2.3.1. *Reactor setup and heating*

Solid, granular sodium salts were placed in the alumina crucible and tube. The electrodes were inserted into the top of the reactor and lowered above the melt. The loaded alumina crucible was positioned in the bottom of the reactor, the lower part of the reactor was raised into place and the flange was closed. The ceramic purge port was secured 20–30 cm above the material in the crucible while the sheathed thermocouple was positioned 1 cm from the bottom of the smelt crucible. The system was purged with argon (0.5–1.2 L_{STP} min^{-1} for the outer system (I, Figure 2), 0.05–0.15 L_{STP} min^{-1} for the tube (J, Figure 2)) for 3 h before heating. The electrochemical cell was heated at approximately 100 °C h^{-1} to the operating temperature (±5 °C).

2.3.2. *Cyclic voltammetry*

The working electrode for the configuration in Equation 16 was flattened platinum wire with a geometric surface area of 1.4 cm^2 exposed to the melt. The working electrode for the MCRE was a platinum wire of 0.0254 cm diameter extending 0.5 cm into the melt. The counter electrode was the same material as the working but with at least an order of magnitude greater

available surface area, achieved by coiling the wire into a tight spiral. The voltammograms were IR-compensated by positive feedback from an EG&G model 263A potentiostat (EG&G, Oak Ridge TN). The potential between the working and the reference was allowed to stabilize about 15 min before a scan was initiated. Scan rates ranged from 0.05 to 1 V s^{-1}. Starting from the open circuit voltage (OCV), the potential was scanned to predetermined values. The data were acquired using a personal computer (National Instruments data acquisition hardware, M270 software developed by EG&G).

3. Results and discussion

The carbonate oxidation allows us a secondary reference point when evaluating the cyclic voltammograms in the cases where the reference electrode experiences potential shifting due to compositional changes. The potential spans presented in the voltammograms are the observed potentials occurring between the working and reference; they have not been shifted to normalize to a standard reference. The significance of the reference reaction shift can be seen by noticing the different locations of carbonate oxidation, indicated by the designation A3, in Figures 3, 6 and 7. Minh and Yao [12] also note that their rest potential of the working electrode becomes more anodic as the concentration of sulfide is increased, which may be attributed to an increased activity of polysulfides in their melt.

The carbonate reaction (Equation 1), with its standard potential of 0 V, is indicated with the designation A3 on the CVs to simplify comparisons to other standard potentials. Gas evolution data from electrolysis experiments show anodic evolution of carbon dioxide while sulfur gases are not detected. Since the only source of carbon in the multicomponent mixture is carbonate, we conclude the reaction at the anodic limit is carbonate oxidizing to carbon dioxide and oxygen.

When sulfide species are present, they rapidly react with the oxygen to form alkali oxy-sulfur species (e.g., Equation 8) and,

$$\tfrac{3}{2}O_2 + Na_2S \rightarrow Na_2SO_3 \qquad K_{900\,^\circ C} = 2.35\times10^{19} \tag{20}$$

while sodium polysulfide in the presence of oxygen and carbonate will eventually become sulfate and carbon dioxide,

$$\tfrac{7}{2}O_2 + Na_2S_2 \rightarrow Na_2S_2O_7 \qquad K_{900\,^\circ C} = 4.57\times10^{37} \tag{21}$$

$$Na_2S_2O_7 + Na_2CO_3 \rightarrow Na_2SO_4 + CO_2 \qquad K_{900\,^\circ C} = 2.97\times10^{10} \tag{22}$$

Off-gas analysis during electrolysis experiments did not reveal any detectable sulfur species by either (a) gas chromatography or (b) inductively coupled plasma (ICP) analysis of a hydrogen peroxide solution that the off-gas was bubbled through. We conclude, therefore, that the sulfur species remained in the molten salt phase.

3.1. *Cyclic voltammetry in a simulated kraft smelt (initial condition for the proposed electrolytic causticizing)*

The kraft smelt recovered from the bottom of the recovery boiler (Figure 1) has a composition dominated by sodium carbonate where the remaining chemicals are sulfur species (typically the composition of Na_2CO_3: Na_2S + Na_2SO_4 ranges from 1:1 to 4:1, mole basis). Here, we verify electroanalytically that carbonate oxidizes according to Equation 1, sulfide oxidizes to polysulfide (Equation 3) and sulfate reduces to oxide and sulfide (Equations 9–12) in a mixture of sodium carbonate (13.5×10^{-3} mol cm^{-3}) and sodium sulfide (3.4×10^{-3} mol cm^{-3}), determined by titration, with minor components of sodium sulfate and polysulfide (2.1×10^{-3} mol cm^{-3}), determined by difference. The presence of sulfide in the melt dramatically changes the characteristics of the voltammogram in comparison to the sodium carbonate/sodium sulfate system [3], where the only peaks between the main reduction and oxidation are reoxidation of oxide and rereduction of carbon dioxide and oxygen. In the system at hand, rereduction of carbon dioxide and oxygen is not observed; anodically produced oxygen rapidly reacts with sodium sulfide to form sodium sulfate (Equation 8).

Figures 3–5 are cyclic voltammograms of the mixture described above at 840 ± 5 °C, scanned at 0.1 V s^{-1} on platinum electrodes in the Pt/PtS configuration. Figure 3 is the first experiment performed on a fresh melt. The OCV is located closer to carbonate oxidation (A3) than in the scan in Figure 4, due to the initially low concentration of polysulfides in the melt. Figure 4 presents scans from the 2nd, 8th and 9th sets of CVs performed. The OCV shifted in a negative direction between the 2nd and 8th/9th experiments, approaching the theoretical span of 1.1 V between carbonate oxidation and the polysulfide/platinum sulfide reference (Equation 18) due to electrochemical reactions changing the oxide, sulfide and polysulfide activities.

Figure 3 also shows that the span between the oxidation and reduction (1.7 V) at the limits of the potential window is shorter than in pure carbonate melts (2.6 V). We are confident that carbonate oxidation is involved in the limiting reaction since carbon dioxide is evolved anodically in electrolysis experiments, to be reported in a future communication. Further, current fluctuations are observed positive of the indicator A3, suggesting gas evolution and bubbling. The span from carbonate oxidation (A3) to the reduction coincides with the prediction of sulfate reduction to sulfide and oxide (Equations 9–12) where two of the steps are indicated by designations C3 and C4.

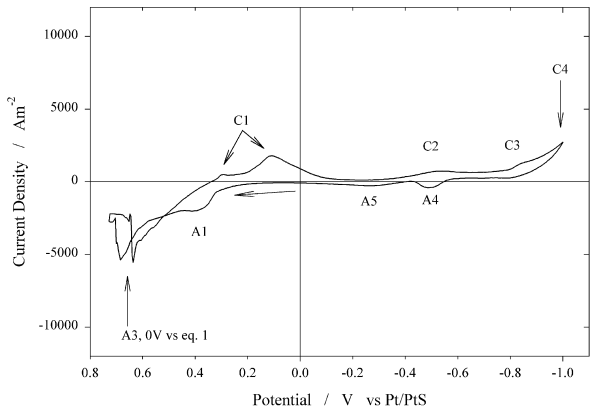

Fig. 3. First scan of a CV experiment for a mixture of Na_2CO_3, Na_2S with impurities of Na_2SO_4 and Na_2S_2. CV was performed at 0.1 V s^{-1} on platinum electrodes at 840 °C under an argon purge. The electrochemical reactions associated with features are summarized in Table 1. Excessive current fluctuations occurred positive of A3, which is carbonate oxidation. An approximate location is given for carbonate oxidation (Equation 1) to facilitate reference to the standard potentials given in the text.

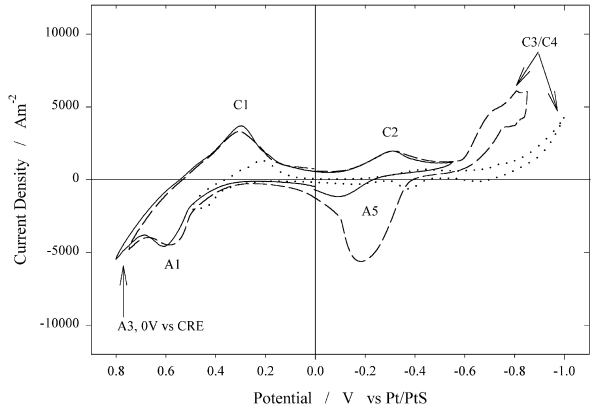

Fig. 4. 2nd (dots), 8th (dash) and 9th (solid) scans of a CV experiment for a mixture of Na_2CO_3, Na_2S with impurities of Na_2SO_4 and Na_2S_2. CVs performed at 0.1 V s^{-1} on platinum electrodes at 840 °C under an argon purge. Increase of sulfate between the 2nd and 8th experiments is evident by the increase in C3/C4.

The first anodic peak encountered (A1) when scanning positive of the OCV, as in Figure 4, is attributed to sulfur formation (Equation 3) (and subsequently polysulfide (Equation 4)) by sulfide oxidation. Polysulfide reoxidation is responsible for the features indicated by C1; the relation to the anodic peak A1 is observed in Figure 4. This polysulfide reduction is consistent with previous findings [6].

The first cathodic peak encountered negative of the OCV, C2, is considered to be peroxide reduction to oxide (Equation 6, $E^{\circ}_{900\,^{\circ}C} = -0.878$ V versus carbonate oxidation) since it is 0.8 to 0.9 V negative of carbonate oxidation (Figures 3 and 4). The reverse of the peroxide reduction occurs as the anodic peak A5 as can be seen by the various extensions into the cathodic regime in Figure 4. It is possible that direct polysulfide reduction to sulfide also occurs at this potential:

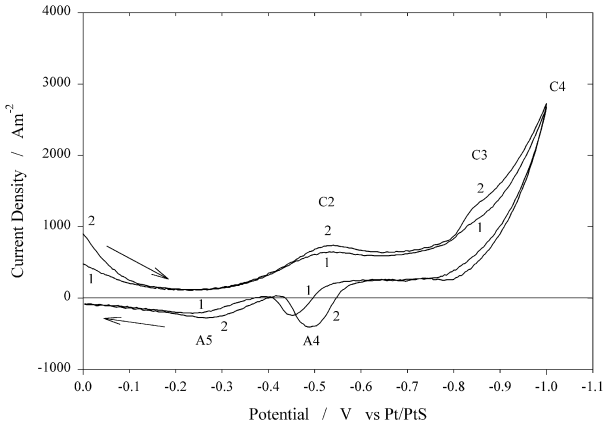

Fig. 5. This Figure shows the reduction branch of the first and second cycles for the CV experiment shown in Figure 3. The CV was performed at 0.1 V s^{-1} on platinum electrodes at 840 °C under an argon purge. Increase of sulfate from oxygen generated by Equation 1 reacting with sulfide is shown by the increase in peaks C3 and C4 of the second cycle.

$$S_2^{2-} + 2\,e^- \leftarrow 2\,S^{2-} \qquad E^{\circ}_{900\,^{\circ}C} = -0.988\,V \tag{23}$$

The sulfate reduction sequence (Equations 9–12) is comprised of peaks C3 and C4 (Figures 3–5). Intermediates are strongly suggested by the disappearance of peak A4 above 0.5 V s^{-1}. Peak A5 consists of multiple oxide oxidations including oxide to oxygen (Equation 5, $E^{\circ}_{900\,^{\circ}C} = -0.888$ V), oxide to peroxide (Equation 6, $E^{\circ}_{900\,^{\circ}C} = -0.878$ V), and peroxide to oxygen (Equation 7, $E^{\circ}_{900\,^{\circ}C} = -0.791$ V). Figure 4 shows how these peaks overlap where the reoxidation of reduction products from C3/C4 encompasses the reoxidation of reduction product from C2. Although sulfate was not directly added to the melt, the observed current at C4, although not a peak, is consistent in magnitude with the concentration based upon the impurities in the sulfide (2.1×10^{-3} mol cm^{-3}) calculated by the Randles–Sevcik equation [13] as 0.5×10^{-3} mol cm^{-3}, where the diffusion coefficient of the same species, D_R, is assumed to be 1.0×10^{-5} cm^2 s^{-1}. Increased currents on subsequent cycles of the same experiment indicate the production of both peroxide and sulfate. This effect can be seen in Figure 5 where the first and second cycles of the first experiment are overlaid onto each other.

3.2. *Cyclic voltammetry in synthetic melts of intermediate and near final conversion for the proposed electrolytic causticizing concept*

Understanding the electrochemical reactions involving sodium oxide, a desired product, is needed for the design of an industrial electrochemical process. Additions of sodium oxide to the melt are expected to increase certain peak heights of the features in the CVs. Solubilities of oxides in our mixtures are not known and may have an effect on the observed current. If oxide oxidations (causing a loss of the desired product) occur before the oxidation at the limit of the potential window, as

thermodynamics predicts and as we will show experimentally below, then a divided electrochemical cell will be necessary in the industrial process design.

3.2.1. *Mixture investigation of $Na_2CO_3/Na_2S_{1,x}/Na_2SO_4$ with additions of Na_2O/Na_2O_2*

Figure 6 is a CV on platinum electrodes scanned at 0.1 V s^{-1} for a melt at a temperature of 820 ± 5 °C. A small amount (0.5×10^{-3} mol cm^{-3}) of sodium oxide/peroxide had been added to it five hours earlier. The composition of the melt was determined by quenched sample titration ($\pm 0.5 \times 10^{-3}$ mol cm^{-3}) one hour after the addition: Na_2CO_3: 16.4×10^{-3} mol cm^{-3}; Na_2S: 2.8×10^{-3} mol cm^{-3}; Na_2O/Na_2O_2: 0.3×10^{-3} mol cm^{-3}; Na_2SO_4/Na_2S_2: 0.2×10^{-3} mol cm^{-3}. The chemicals initially loaded into the cell were sodium carbonate (15.1×10^{-3} mol cm^{-3}), and sodium sulfide (4.0×10^{-3} mol cm^{-3}). Sodium sulfate and sodium polysulfides are present as impurities (0.5×10^{-3} mol cm^{-3}) and the sodium oxide composition is Na_2O: 0.4×10^{-3} mol cm^{-3}, Na_2O_2: 0.1×10^{-3} mol cm^{-3}, based on the manufacturer's assay. The OCV in Figure 6 had shifted in a negative direction when compared to Figures 3 and 4 indicating a change to the Pt/PtS reference.

In Figure 6, no significant oxidation current is observed until A1, which is attributed to sulfide oxidation to sulfur (Equation 3). Sulfur will chemically react with additional sulfide to form polysulfide (Equation 4), as in the previous system without added oxide. Peak A2 is also considered to represent further formation of polysulfides. Again we notice the rereduction of polysulfides by the peaks under C1. Carbonate oxidation at A3 is about 0.9 V from the reference indicating the reference electrode's shift toward its theoretical value of −1.1 V for the Pt/PtS reference. Oxidation current is not observed before peak A1 as would be expected from oxide oxidations (Equations 5–7). This is attributed to the significant time (~5 h) between the oxide addition and the scans allowing for oxide-consuming chemical reactions including fluxing with alumina.

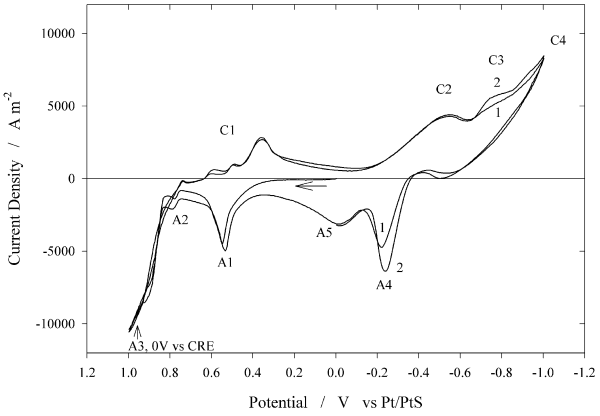

Fig. 6. Two cycles of a CV experiment for a mixture of Na_2CO_3, Na_2S with impurities of Na_2SO_4 and Na_2S_2 where an addition of Na_2O/Na_2O_2 was made five hours before. The CV was performed at 0.1 V s^{-1} on platinum electrodes at 820 °C under an argon purge.

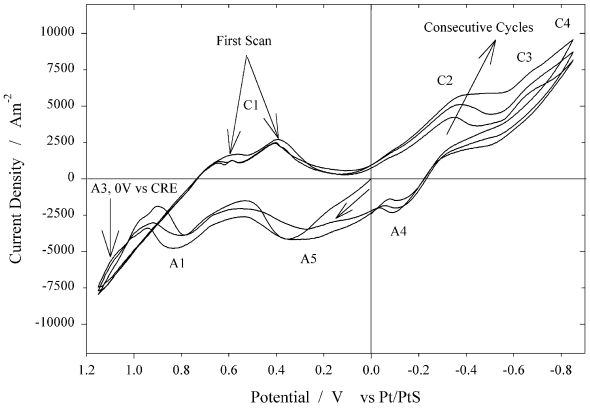

Fig. 7. CV experiment for a mixture of Na_2CO_3, Na_2S with impurities of Na_2SO_4 and Na_2S_2 where a large addition of Na_2O/Na_2O_2 has been made (4 to 5 times as large as the addition made to the system described by Figures 6–9). The CV was performed at 0.1 V s^{-1} on platinum electrodes at 840 °C under an argon purge. Oxidation current is immediately observed at A5 when the scan is started positive indicating oxide oxidation.

Figure 7 shows the results for the same system as in the initial melt of Figures 3–5, with an oxide addition of Na_2O: 2.3×10^{-3} mol cm^{-3}, Na_2O_2: 0.4×10^{-3} mol cm^{-3}. The cyclic voltammogram in Figure 7 was taken one half-hour after the addition of sodium oxide/peroxide. The anodic reaction A3, attributed to carbonate oxidation, is about 1.1 V positive of the OCV indicating the reference is behaving as a Pt/PtS electrode. The potential span between the anodic and cathodic limits fits the thermodynamic prediction of carbonate oxidation (Equation 1) and sulfate reduction (Equations 9–12) of about 1.8 V. The CV presented in Figure 7 begins in the positive direction; anodic current is immediately realized due to oxide and peroxide oxidation (Equations 5–7). This peak occurrence is important because it shows that CV can indicate the presence of oxides in a mixture. This effect can be observed when comparing Figure 7 (with significant oxides) and Figures 3–6 which either did not have oxides or had the oxides consumed before the scan. Oxide and peroxide oxidation ultimately result in oxygen evolution that drives sodium oxide to sodium peroxide (Equation 6) increasing peak C2 in subsequent cycles. Oxygen also chemically oxidizes sulfide to sulfate (Equation 8) and consequently increases electrochemical sulfate reduction in peaks C3 and C4.

3.2.2. *Investigation of a 'near-final' mixture*

For the purpose of electrochemical recausticizing, it is necessary to know what electrochemical reactions will dominate contributions to the current under electrolysis conditions, not only at the beginning of the process (Na_2CO_3, Na_2S and Na_2SO_4), but also at the end where the melt is high in desired sodium oxide and sodium sulfide.

Figures 8 and 9 are CVs on platinum electrodes for a mixture of predominantly sodium oxide (12.0×10^{-3} mol cm^{-3}) and peroxide (1.7×10^{-3} mol cm^{-3}), sodium

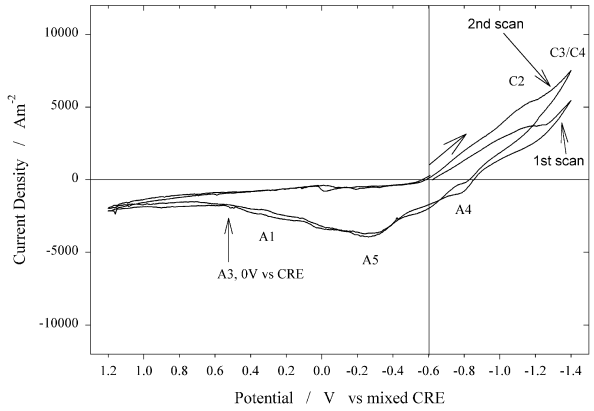

Fig. 8. CV experiment for a mixture composed to have a near final conversion containing Na_2O/Na_2O_2, Na_2S with minor constituents of Na_2CO_3 and Na_2SO_4. CV initiated in the cathodic direction at 0.1 V s^{-1} on platinum electrodes at 824 °C under an argon purge.

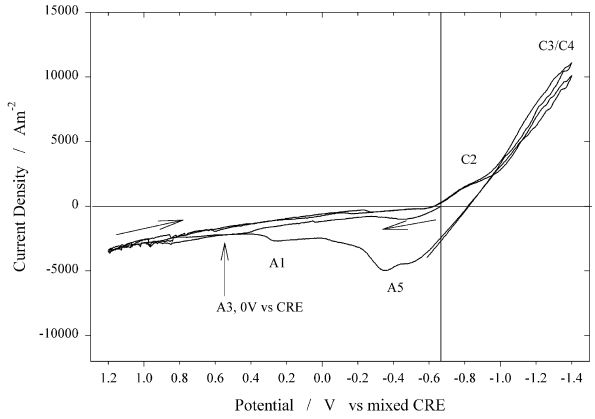

Fig. 9. CV experiment for a mixture composed to have a near final conversion containing Na_2O/Na_2O_2, Na_2S with minor constituents of Na_2CO_3 and Na_2SO_4. The CV was initiated in the anodic direction at 0.1 V s^{-1} on platinum electrodes at 824 °C under an argon purge.

sulfide (6.7×10^{-3} mol cm^{-3}) [which contained up to 0.6×10^{-3} mol cm^{-3} of sodium polysulfide and sodium sulfate] with minor components of sodium carbonate (3.8×10^{-3} mol cm^{-3}), and sodium sulfate (1.0×10^{-3} mol cm^{-3}) at 824 °C (scan rate 0.1 V s^{-1} unless otherwise noted). Equation 17 indicates the electrode configuration used for these experiments. The CVs were compared to the data from other mixtures based upon features of the scan and location of the OCV of the cell assuming the MCRE reference electrode controlled it.

Figure 8 begins in a reducing direction and shows peroxide reduction to oxide, peak C2, has increased when compared to the initial melt with no oxide added (Figure 3). The reduction at the limit of the potential window is attributed to the sulfate reduction series involving C3/C4 while peaks A4 (oxidation of sulfate reduction intermediates, Equations 9–11) and A5 (family of oxide oxidations, Equations 5–7) are consequently observed. A shoulder is noticed at 0.2–0.3 V negative of carbonate oxidation in both Figures 8 and 9, corresponding to sulfide oxidation to sulfur (A1, Equation 3) and subsequent chemical reaction to polysulfide (Equation 4). Yet, we do not observe polysulfide rereduction since either (a) polysulfide has reacted with oxide to form peroxide and sulfide or (b) sulfur from Equation 3 (A1) reacted with oxide and oxygen to form sulfate.

Due to decreased sodium carbonate activity we do not observe a steep carbonate oxidation (Equation 1) in Figures 8 and 9 as we do in Figure 3. Carbonate oxidation has been confirmed in the near-final compositions since electrolysis experiments detect carbon dioxide from anodic chambers of similar melts (to be reported elsewhere). The oxide oxidations (Equations 5–7, peak A5) contribute to a majority of the current within the limits of the potential window. Significantly smaller oxidation currents in the vicinity of A5 (oxide oxidations, Equations 5–7) are observed when the scan is initiated in the oxidizing direction (Figure 9). This supports the idea of a maximum solubility limit for sodium oxide or a chemical equilibrium affecting sodium oxide because the peak height of A5 does not increase proportionally to the oxide concentration.

Table 1. Summary of electrochemical reactions determined by CV and their standard potentials against carbonate oxidation

Peak designation	Electrochemical reaction	Standard potential, versus Equation 1 $E^{\circ}_{900\,^{\circ}C}$ V	Equation
A1/A2	$S^{2-} \rightarrow \frac{1}{2}S_2 + 2e^-$	−0.701	3
A3	$CO_3^{2-} \rightarrow CO_2 + \frac{1}{2}O_2 + 2e^-$	0	1
C1	$S^{2-} \rightarrow \frac{1}{2}S_2 + 2e^-$, and polysulfides	−0.701	3
C2	$O_2^{2-} + 2e^- \rightarrow 2O^{2-}$	−0.878	6
	$S_2^{2-} + 2e^- \rightarrow 2S^{2-}$ (possible)	−0.988	22
C3/C4	$SO_4^{2-} + 2e^- \rightarrow SO_3^{2-} + O^{2-}$	−1.822	8
	$SO_3^{2-} + 2e^- \rightarrow SO_2^{2-} + O^{2-}$		9
	$SO_2^{2-} + 2e^- \rightarrow \frac{1}{2}S_2^0 + 2O^{2-}$		10
A4	$SO_3^{2-} + O^{2-} \rightarrow SO_4^{2-} + 2e^-$	−1.882	8
	$SO_2^{2-} + O^{2-} \rightarrow SO_3^{2-} + 2e^-$		9
	$\frac{1}{2}S_2^0 + 2O^{2-} \rightarrow SO_2^{2-} + 2e^-$		10
A5	$O^{2-} \rightarrow \frac{1}{2}O_2 + 2e^-$	−0.888	5
	$2O^{2-} \rightarrow O_2^{2-} + 2e^-$	−0.878	6
	$O_2^{2-} \rightarrow O_2 + 2e^-$	−0.791	7

4. Conclusions

Molten mixtures containing sodium carbonate, sulfide, sulfate and oxides have been investigated using CV and are summarized in Table 1. In all mixtures, carbonate oxidation occurs at the positive voltage limit, and sulfate reduction at the negative limit. At intermediate potentials oxidations and reductions of oxide species are present and identified, as are those of sulfide. Oxygen released during the oxidations results in the undesirable conversion of sulfide to sulfate. Therefore an industrial design for the conversion of carbonate to oxide in the presence of sulfide will require a divided cell, with a separator permeable to sodium ions, but retaining oxide ions in the cathode chamber. Such sodium ion conductors are available since they have been developed for high-temperature sodium batteries. With such a selective barrier in place, the main electrochemical reactions will be the generation of sodium oxide and sulfide from sulfate in the catholyte and the evolution of carbon dioxide and formation of polysulfide from carbonate and sulfide, respectively, in the anolyte. The fundamental electrochemical behavior described here opens a number of options for the technical realization of this process.

Acknowledgements

The authors would like to thank the United States Department of Energy (DE-FC07-97ID13547) and the member companies of the Institute of Paper Science and Technology for their financial support.

References

1. American Forest and Paper Association, 'Statistics of Paper, Paperboard and Wood Pulp', Technical Report, American Forest and Paper Association, Washington, DC (1994).
2. T.M. Grace, B. Leopold and E.W. Malcolm, Alkaline Pulping, *in* M.J. Kocurek and F. Stevens (Eds), 'Pulp and Paper Manufacture' Vol. 5, Joint Textbook Committee of the Paper Industry of the United States and Canada, Atlanta (1991), p. 367.
3. R. Wartena, J. Winnick and P.H. Pfromm, *J. Appl. Electrochem.*, **32** (2002) 415–424.
4. D.R. Jr. Lide, Editor, 'Journal of Physical and Chemical Reference Data, JANAF Thermochemical Tables' (American Institute of Physics, New York, 1986).
5. K.K. Kelley and C.T. Anderson, 'Contributions to the Data on Theoretical Metallurgy: IV. Metal Carbonates – Correlations and Applications of Thermodynamic Properties' Bulletin 384 (US Department of the Interior, Bureau of Mines, Washington, DC 1935).
6. R.P. Tischer, 'The Sulfur Electrode: Fused Salts and Solid Electrolytes' (Academic Press, New York, 1983) p. 375.
7. B.K. Andersen, 'Thermodynamic Properties of Molten Alkali Carbonates', Dissertation (Technical University of Denmark, Lyngby, 1975).
8. R.A. Rapp and K.S. Goto, *in* J. Braunstein and J.R. Selman (Eds),'Hot Corrosion of Metals by Molten Salts', Proceedings of the Second International Symposium on Molten Salts, Pittsburgh, PA, Oct. (1978), p. 159–177.
9. C.A.C. Sequeira and M.G. Hocking, *Electrochim. Acta* **23** (1978) 381–388.
10. G.J. Janz, 'Molten Salts Handbook' (Academic Press, New York, 1967) p. 588.
11. L.W. Tilton, *J. Am. Ceram. Soc.* **43** (1) (1960) 9–17.
12. A.J. Bard and L.R. Faulkner, 'Electrochemical Methods: Fundamentals and Applications', (J. Wiley & Sons, New York, 1980), p. 718.
13. N.Q. Minh and N-P. Yao, *J. Electrochem. Soc.* **130** (5) (1983) 1025–1029.